Physica D 460 (2024) 134056

Contents lists available at ScienceDirect

Physica D

journal homepage: www.elsevier.com/locate/physd

Stability and dynamics of regular and embedded solitons of a perturbed Fifth-order KdV equation

S. Roy Choudhury [a], Gaetana Gambino [b,*], Ranses Alfonso Rodriguez [c]

[a] Department of Mathematics, University of Central Florida, Orlando, FL 32816, USA
[b] Department of Mathematics and Computer Science, University of Palermo, Via Archirafi 34, 90123 Palermo, Italy
[c] Department of Applied Mathematics, Florida Polytechnic University, Lakeland, FL 33805, USA

ARTICLE INFO

Communicated by He Jingsong

Keywords:
Regular and embedded solitons
Stability and dynamics
Perturbative and infinite series
Fifth-order kdV equation

ABSTRACT

Families of symmetric embedded solitary waves of a perturbed Fifth-order Korteweg–de Vries (FKdV) system were treated in Choudhury et al. (2022) using perturbative and reversible systems techniques. Here, the stability of those solutions, which was not considered in the earlier paper, is detailed. In addition, the results of Choudhury et al. (2022) are extended to the case of asymmetric solitary waves, as well as their stability. Finally, other novel multi-humped regular solitary waves of this system are derived using convergent infinite series solutions for the homoclinic orbits of the FKdV-traveling wave equation.

1. Introduction

The Korteweg–de Vries (KdV) equation

$$\frac{\partial v}{\partial t} + c\frac{\partial v}{\partial x} + \alpha v\frac{\partial v}{\partial x} + \beta\frac{\partial^3 v}{\partial x^3} = 0, \tag{1.1}$$

is a very well-known model for the description of weakly-nonlinear long waves (in shallow water) in media with small dispersion (see, for instance, [1–3]). It is employed in the theory of long internal waves, and describes the main properties of even large-amplitude nonlinear waves. It has also been employed as the earliest and simplest model incorporating both nonlinear and dispersive effects, and has both periodic and solitary wave solutions. The KdV equation is completely integrable, and possesses many remarkable properties, which are summarized in the references cited above.

However, the KdV equation does not include many important features of nonlinear waves observed in experiments, such as the large-amplitude flat-top solitary waves or the non-monotonic dependence of their wave speed on amplitude [4]. The first natural extension of the KdV model retains the next-order nonlinear and dispersive terms in the asymptotic expansion of the solutions to the full Euler equations, with boundary conditions appropriate for oceanographic applications in the case of the ocean gravity waves. Many authors [5–7] have considered the extended fifth-order KdV equation:

$$\frac{\partial v}{\partial t} + c\frac{\partial v}{\partial x} + \alpha_1 v\frac{\partial v}{\partial x} + \beta_1\frac{\partial^3 v}{\partial x^3} + \epsilon\left(\alpha_2 v^2\frac{\partial v}{\partial x} + \gamma_1 v\frac{\partial^3 v}{\partial x^3} + \gamma_2\frac{\partial v}{\partial x}\frac{\partial^2 v}{\partial x^2} + \beta_2\frac{\partial^5 v}{\partial x^5}\right) = 0. \tag{1.2}$$

This equation, written in a coordinate frame moving with the speed c, combines the quadratic ($\sim \alpha_1$) and cubic ($\sim \alpha_2$) nonlinear terms, linear dispersion of the third ($\sim \beta_1$) and fifth ($\sim \beta_2$) orders, and also higher-order nonlinear dispersion terms with coefficients γ_1 and γ_2; the expansion parameter $\epsilon \ll 1$ is presumed to be small.

Particular cases of the fifth-order KdV equation, with one or more coefficients being zero, have also been derived in a variety of applications [8,9].

In general, Eq. (1.2) is not integrable, but for particular choices of coefficients it reduces to one of a set of equations that are completely integrable. These are the Gardner equation (when $\beta_2 = \gamma_1 = \gamma_2 = 0$) or its particular case the standard KdV/mKdV equation (when either $\alpha_1 = 0$ or $\alpha_2 = 0$), as well as the Sawada–Kotera and Kaup–Kupershmidt equations (when $\alpha_1 = \beta_1 = 0$) [3].

Unlike the KdV equation, the higher-order model (1.2) is not a Hamiltonian equation and does not, in general, preserve the energy. However, in the particular cases when it reduces to completely integrable models, it clearly becomes Hamiltonian.

Many other properties of the higher-order models are discussed and summarized in [9–11].

In this paper we will analyze the following FKdV equation:

$$\frac{\partial v}{\partial t} + \alpha_1 v\frac{\partial v}{\partial x} + b\frac{\partial^3 v}{\partial x^3} + \alpha_2 v^2\frac{\partial v}{\partial x} + \alpha_3 v\frac{\partial^3 v}{\partial x^3} + \alpha_4\frac{\partial v}{\partial x}\frac{\partial^2 v}{\partial x^2} + a\frac{\partial^5 v}{\partial x^5} = 0, \tag{1.3}$$

where we have used the roman letters a, b for the coefficients of linear terms and $\alpha_j, j = 1, \ldots 4$ are the coefficients of the nonlinear terms. All the coefficients are real.

* Corresponding author.
E-mail address: gaetana.gambino@unipa.it (G. Gambino).

https://doi.org/10.1016/j.physd.2024.134056
Received 6 October 2023; Received in revised form 8 December 2023; Accepted 11 January 2024
Available online 18 January 2024

Families of symmetric embedded solitary waves of this system were recently derived in [11] using a combination of perturbative and reversible systems techniques in a manner analogous to [10]. Here we will consider the stability of those solutions, which was not done in the earlier paper. In addition, we will extend the results of [11] to the case of asymmetric solitary waves, and the stability of these solitary structures will be also addressed. Finally, we will employ infinite series solutions for the homoclinic orbits of the FKdV-traveling wave equation to derive convergent multi-humped solitary waves of this system.

Section 2 considers the traveling waves of (1.3), including the bifurcation of possible solutions as the system parameters are varied. This lays the groundwork for both the perturbative solitary wave solutions, as well as those derived subsequently using multi-infinite series. Section 3 briefly summarizes the results of [11], while Sections 4 and 5 employ them to derive embedded soliton solutions. Section 6 then significantly generalizes the results of [11] to the case of asymmetric nonlocal solitary waves. Next, Section 7 considers the dynamics and stability of both symmetric and asymmetric embedded solitons in detail. Note that [11] did not treat asymmetric solitary waves at all, and did not consider the dynamics and stability of either the symmetric or asymmetric embedded solitons. Section 8 then derives other families of regular solitary waves using multi-infinite series, and many numerical tests are performed in different parameter regimes to corroborate the analytical results, showing the convergence and continuity of the multi-infinite series solutions. Finally, Section 9 summarizes the results of the paper. A few key background results from [11] are summarized in the Appendixes.

2. Traveling wave equation and bifurcation analysis

The Eq. (1.3) can be written in the following form:

$$\frac{\partial v}{\partial t}+\frac{\partial}{\partial x}\left[\alpha_1\frac{v^2}{2}+b\frac{\partial^2 v}{\partial x^2}+\alpha_2\frac{v^3}{3}+\alpha_3 v\frac{\partial^2 v}{\partial x^2}+\frac{(\alpha_4-\alpha_3)}{2}\left(\frac{\partial v}{\partial x}\right)^2+a\frac{\partial^4 v}{\partial x^4}\right]=0, \tag{2.1}$$

We look for stationary traveling wave solutions. Substituting

$$v(\zeta)=v(x-ct) \tag{2.2}$$

in (2.1), integrating one time with respect to ζ and setting the constant of integration to zero, we obtain:

$$av''''+bv''-cv=-\alpha_1\frac{v^2}{2}-\alpha_2\frac{v^3}{3}-\alpha_3 vv''+\frac{(\alpha_3-\alpha_4)}{2}v'^2 \tag{2.3}$$

where $'=\frac{d}{d\zeta}$.

The Eq. (2.3) is invariant under the transformation $\zeta\to-\zeta$, which means that it is a reversible system [12].

The equilibria of Eq. (2.3) are the solutions of the following equation:

$$\alpha_2\frac{v^3}{3}+\alpha_1\frac{v^2}{2}-cv=0, \tag{2.4}$$

therefore the trivial equilibrium exists for any choice of the parameters:

$$v=v'=v''=v'''=0. \tag{2.5}$$

If $\alpha_2=0$ there exists also the equilibrium $v=-2c/\alpha_1$; if $\alpha_2\neq 0$ and $9\alpha_1^2+48\alpha_2 c>0$, the following two equilibria also exist in addition to the origin:

$$v_\pm^*=\frac{-3\alpha_1\pm\sqrt{9\alpha_1^2+48\alpha_2 c}}{4\alpha_2}. \tag{2.6}$$

These will be considered further later in the context of multi-infinite solutions, including possible heteroclinic connections or orbits joining one of these equilibria to the other.

We linearize Eq. (2.3) as follows:

$$av''''+bv''-cv=0. \tag{2.7}$$

whose corresponding characteristic equation is:

$$a\lambda^4+b\lambda^2-c=0. \tag{2.8}$$

The solutions of Eq. (2.8), and consequently the solutions of Eq. (2.3), strictly depend on the value of the discriminant $\Delta=b^2+4ac$ and on the sign of the coefficients a, b and c. Restricting our interest to the case $a\neq 0$ (in fact we are considering a fifth order KdV equation), we can distinguish the following cases:

- (i) $b=c=0$: all the eigenvalues are equal to zero $\lambda_1=\lambda_2=\lambda_3=\lambda_4=0$.
- (ii) $c=0$ and
  - $(ii.1)$ $a,b\neq 0$ of the same sign: Eq. (2.8) admits the solutions $\lambda_1=\lambda_2=0$, $\lambda_{3-4}=\pm i\sqrt{-\frac{b}{a}}$;
  - $(ii.2)$ $a,b\neq 0$ of opposite sign: Eq. (2.8) admits the solutions $\lambda_1=\lambda_2=0$, $\lambda_3=\sqrt{-\frac{b}{a}}\in\mathbb{R}^+$ and $\lambda_4=-\sqrt{-\frac{b}{a}}\in\mathbb{R}^-$.
- (iii) $\Delta=0$, $c\neq 0$ and
  - $(iii.1)$ $a,b\neq 0$ of the same sign: Eq. (2.8) admits the solutions $\lambda_1=\lambda_2=i\sqrt{-\frac{b}{2a}}$ and $\lambda_3=\lambda_4=-i\sqrt{-\frac{b}{2a}}$;
  - $(iii.2)$ $a,b\neq 0$ of opposite sign: Eq. (2.8) admits the solutions $\lambda_1=\lambda_2=\sqrt{-\frac{b}{2a}}\in\mathbb{R}^+$ and $\lambda_3=\lambda_4=-\sqrt{-\frac{b}{2a}}\in\mathbb{R}^-$.

In what follows, to better understand the behavior of the solutions of the characteristic equation (2.8) as described above, we fix the coefficient a and display the bifurcation diagram Figure 1(a) corresponding to the linearized equation (2.7) in the plane (b,c). Analogously, we then fix the parameter b and draw the bifurcation diagram Figure 1(b) in the plane (a,c). The conditions (i)–(iii) will arise along codimension-one curves in the (b,c) or (a,c) plane.

CASE 1: Let the parameter a be fixed. We define the following co-dimension one curves:

$$\text{If a} > 0: \quad C_0: c=0,\ b>0, \quad C_1: c=0,\ b<0, \quad C_2: c=-\frac{b^2}{4a},\ b>0, \quad C_3: c=-\frac{b^2}{4a},\ b<0; \tag{2.9}$$

$$\text{If a} < 0: \quad C_0: c=0,\ b<0, \quad C_1: c=0,\ b>0, \quad C_2: c=-\frac{b^2}{4a},\ b<0, \quad C_3: c=-\frac{b^2}{4a},\ b>0. \tag{2.10}$$

CASE 2: Let the parameter b be fixed. We assume $b>0$. We define the following co-dimension one curves:

$$\text{If b} > 0: \quad C_0: c=0,\ a>0, \quad C_1: c=0,\ a<0, \quad C_2: ac=-\frac{b^2}{4},\ a>0, \quad C_3: ac=-\frac{b^2}{4},\ a<0; \tag{2.11}$$

$$\text{If b} < 0: \quad C_0: c=0,\ a<0, \quad C_1: c=0,\ a>0, \quad C_2: ac=-\frac{b^2}{4},\ a<0, \quad C_3: ac=-\frac{b^2}{4},\ a>0. \tag{2.12}$$

In both Cases 1 and 2, the curve C_0 is that one along which the eigenvalues are as in $(ii.1)$, the curve C_1 is that one along which the eigenvalues are as in $(ii.2)$, the curve C_2 is that one along which the eigenvalues are as in $(iii.1)$ and, finally, the curve C_3 is that one along which the eigenvalues are as in $(iii.2)$. The eigenvalues are as in (i) at the origin of the plane. In Fig. 1, we display the curves C_i in two illustrative cases. In particular, we choose $a=1$ (corresponding to (2.9)) and $b=1$ (corresponding to (2.11)), respectively. Fig. 1 thus shows the curves along which the eigenvalues of Eq. (2.8) change their structure. In Appendix A we briefly review how this change of structure define the orbits homoclinic to the fixed point of (2.7) which in turn correspond to pulse solitary waves of the FKdV5 equation (1.3).

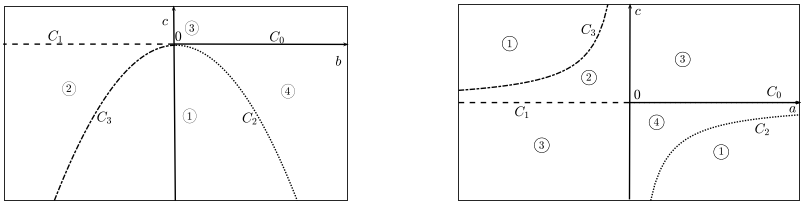

Fig. 1. Bifurcation diagram corresponding to the characteristic equation (2.8). (a) Co-dimension one curve $C_i, i = 0, \dots, 4$ corresponding to definition in (2.9). The parameter $a = 1$. (b) Co-dimension one curve $C_i, i = 0, \dots, 4$ corresponding to definition in (2.11). The parameter $b = 1$.

3. Background theory

In this Section we shall consider the following perturbed FKdV equation:

$$\frac{\partial v}{\partial t} + \alpha_1 v \frac{\partial v}{\partial x} + b\frac{\partial^3 v}{\partial x^3} + c_1 v \frac{\partial^3 v}{\partial x^3} + c_2 \frac{\partial v}{\partial x}\frac{\partial^2 v}{\partial x^2} + c_3 v^2 \frac{\partial v}{\partial x} + a\frac{\partial^5 v}{\partial x^5} = \varepsilon F(v), \quad (3.1)$$

where:

$$F(v) = -\left\{ a_1 v \frac{\partial^3 v}{\partial x^3} + a_2 \frac{\partial v}{\partial x}\frac{\partial^2 v}{\partial x^2} + a_3 v^2 \frac{\partial v}{\partial x} \right\}, \quad (3.2)$$

is the perturbation term with $\varepsilon \ll 1$ and a, b, c_i, a_i are constant coefficients. As in [10], we include perturbations from the integrable case in the dispersion and nonlinearities.

The Eq. (3.1) belongs to the class of Eq. (1.3) with:

$$\alpha_2 = c_3 + \varepsilon a_3, \qquad \alpha_3 = c_1 + \varepsilon a_1, \qquad \alpha_4 = c_2 + \varepsilon a_2. \quad (3.3)$$

Therefore, looking for traveling wave solution $v(\zeta) = v(x - ct)$ and proceeding as in the previous Section 2, we obtain the following fourth-order ODE equation:

$$v'''' + bv'' - cv = -3v^2 - c_3\frac{v^3}{3} - c_1 v v'' + \frac{(c_1 - c_2)}{2} v'^2 + \varepsilon G(v), \quad (3.4)$$

with:

$$G(v) = -\left\{ a_1 v v'' + \frac{1}{2}(a_2 - a_1) v'^2 + \frac{1}{3} a_3 v^3 \right\}. \quad (3.5)$$

In what follows, we shall study nonlocal solitary waves and analytically establish the existence of embedded solitons to Eq. (3.1). To minimize the number of parameters in the problem we will choose the parameter set corresponding to the KdV hierarchy:

$$a = 1, \quad \alpha_1 = 6, \quad c_1 = 10, \quad c_2 = 20, \quad c_3 = 30. \quad (3.6)$$

with wave speeds $c < 0$.

Notice that in [10] the coefficient b was set equal to 1 (corresponding to the third-order dispersive term in the original PDE), while b is left arbitrary here. While that may seem a minor feature, as we shall see in the next sections, it leads to entirely new classes of embedded solitary waves based on perturbations of a disjoint family of solitary wave solutions to the unperturbed equation and existing in completely different regions of the parameter space. Since we have fixed the parameters as in (3.6), the bifurcation analysis of the linearized equation corresponding to (3.4) is given as in Case 1 of Section 2. Notice that we shall restrict our discussions to Regions 1, 2 and 4 in Fig. 1(a) corresponding to $c < 0$.

4. Symmetric nonlocal solitary waves

In this Section we briefly review some essential results on symmetric nonlocal solitary waves solutions from [11]. Some details are reported in Appendix B.

For $0 \neq \varepsilon \ll 1$, we propose the solution v of Eq. (3.4) as a regular perturbation series:

$$v(z) = v_0(\zeta) + \varepsilon v_1(\zeta) + \varepsilon^2 v_2(\zeta) + \varepsilon^3 v_3(\zeta) + \cdots. \quad (4.1)$$

Once substituted (4.1) into (3.4)–(3.5), a family of equations for v_i are obtained at each power of ε. The solution for $v_0(\zeta)$ is obtained as in (B.1). The coefficient $v_1(\zeta)$ (and therefore the solution $v(\zeta)$) is nonlocal, as discussed in Appendix B. At infinity the nonlinear terms decay. Hence, as in [11], these waves behave, asymptotically, as

$$v_1(\zeta) \to \pm R \sin(p\zeta \pm \phi), \qquad \zeta \to \pm\infty, \quad (4.2)$$

where R is the tail amplitude and ϕ is the phase of the nonlocal wave. If we add any multiple of Ψ_3 (given in (B.9)) to v_1, the new function still remains a symmetric nonlocal solution (see Eq. (B.6)). Hence, there must be a free parameter in the v_1 solution. In (4.2), there are two parameters, R and ϕ; however, only one of them is a free parameter.

Going back to Eq. (B.6), and recalling that L is self-adjoint, we find that

$$\langle G(v_0), \Psi_3 \rangle = \left(v_1''' \Psi_3 - v_1'' \Psi_3' + v_1' \Psi_3'' - v_1 \Psi_3''' - b v_1' \Psi_3 + b v_1 \Psi_3' \right)\Big|_{-\infty}^{\infty}. \quad (4.3)$$

Considering only the asymptotic behaviors of v_1 and Ψ_3 [10], we can conclude that

$$R \sin(\phi - \phi_3) = -R \cos(\phi - \phi_2) = \frac{\langle G(v_0), \Psi_3 \rangle}{p(4p^2 - 1 + b)}. \quad (4.4)$$

The formula (4.4) relates the tail amplitude and phase, through the quantity $\langle G(v_0), \Psi_3 \rangle$, which we have already obtained in Eq. (B.16). If $\langle G(v_0), \Psi_3 \rangle \neq 0$, then $R \neq 0$. Therefore the solution v_1, as well as v, is truly nonlocal.

When $\phi - \phi_3 = \pm\pi/2$, or v_1 and Ψ_3 are ninety degrees out of phase, the tail amplitude is smallest, while it has a simple pole singularity and takes its maximum value when $\phi - \phi_3 = \pm\pi$. In the latter case, v_1 and Ψ_3 are exactly in phase or out of phase, as deduced via a resonance explanation for infinite tail amplitudes seen in the numerical treatment in [13]. Higher order corrections to the tail amplitude may be systematically constructed by calculating later terms in our perturbation expansion (4.1).

Eq. (4.4) for the tail amplitude for arbitrary wavespeeds c may be related to similar expressions obtained via exponential asymptotics approaches [13–16] in the limit of small wavespeed c. This may be seen for $c \to 0^-$ and $c < 0$, we have $k \to (c/b)^{1/2}$, $p \to b^{1/2}$, and $\phi_3 - > 0$. Hence, to leading order, (4.4) yields

$$R \sin(\phi) = \frac{-9\pi |b|^{5/2}(1 - b)(2a_1 + a_2 - a_3).e^{-b\pi/|c|^{1/2}}}{5(1 - 5b)}. \quad (4.5)$$

As in [10], we next analyze the existence of truly nonlocal solitary waves and embedded solitons using (4.5).

5. Embedded solitons

When $\langle G(v_0), \Psi_3 \rangle = 0$, that is

$$\begin{aligned} &-2a_3(4k^2 + p^2)(-6 + 125k^2 + p^2 + 5b) \\ &- a_1\left(270k^4 - 4p^2(-6 + p^2 + 5b) + k^2(6 - 476p^2 - 5b)\right) \\ &+ a_2\left(-1270k^4 + 2p^2(-6 + p^2 + 5b) + k^2(42 + 218p^2 - 35b)\right) = 0, \end{aligned} \quad (5.1)$$

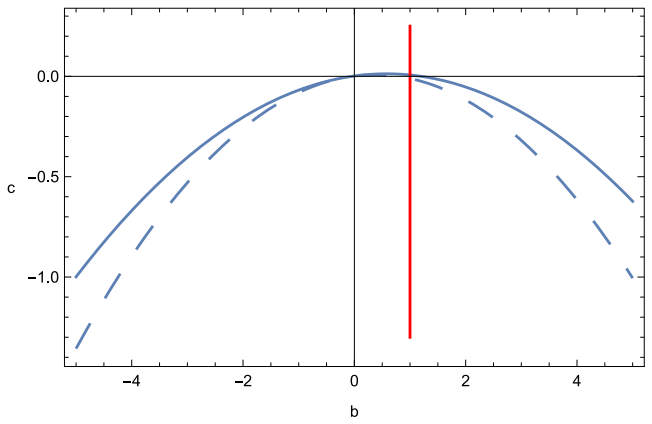

Fig. 2. Isolated curves in the (b, c) plane where solitons can exist. c_2 is shown dashed.

or

$$2(2a_1 + a_2 - a_3)\left[p^4 - p^2(-5b + 6)\right] - (a_1 - 7a_2 - 8a_3)k^2(-5b + 6)$$
$$- 10(27a_1 + 127a_2 + 100a_3)k^4 + 2(238a_1 + 109a_2 - 129a_3)k^2p^2 = 0, \quad (5.2)$$

the tail amplitude R goes to zero. In this case $v_1(\zeta)$ is a localized solution and $v(\zeta)$ is a symmetric solitary wave (to order ε). Higher order corrections in (4.1) may be systematically calculated to slightly modify condition (5.2), while leaving $v(\zeta)$ localized. Although we would need to check this separately, such localized solutions embedded within seas of delocalized solitary waves with non-zero tail amplitudes typically reside within, or are embedded inside, the continuous spectrum of the linearized operator (B.7). Hence they are referred to as embedded solitons, or ES's for short [10,13].

Two distinct cases when condition (5.2) is satisfied can be directly identified, and lead to distinct families of embedded solitons.

1. A one-parameter family of ES's: After some algebra, condition (5.2) may be shown to have solutions with $a_2 = -a_1, a_3 = a_1, p^2 = -k^2 = b/2$, and parametrized by the free variable b. This leads to a family of isolated solitons moving at *arbitrary* wavespeed $c_{\text{family}} = -b^2/4$.

2. Isolated embedded soliton families for two distinguished wavespeeds: When $a_3 = 2a_1 + a_2$, (5.2) yields

$$-5(a_1 + a_2)k^2(454k^2 + 8p^2 - 3(6 - 5b)) = 0. \quad (5.3)$$

Solving for p^2 gives

$$p^2 = \frac{1}{8}(18 - 454k^2 - 15b). \quad (5.4)$$

Then, using that $c = bk^2 + k^4$ and $c = p^4 - bp^2$, or what is the same

$$bk^2 + k^4 - p^4 + bp^2 = 0,$$

we can solve for k^2:

$$k^2 = \frac{3}{446}(6 - 5b), \qquad k^2 = \frac{1}{462}(18 - 23b). \quad (5.5)$$

Therefore, one gets two isolated soliton families moving at wave speeds:

$$c_1 = \frac{3}{446}b(6 - 5b) + \frac{(9(6 - 5b)^2)}{198916}, \qquad c_2 = \frac{1}{462}b(18 - 23b) + \frac{(18 - 23b)^2}{213444}. \quad (5.6)$$

Contrary to the first case, these wave speeds are valid only up through $O(\varepsilon)$, and may be refined by computing further terms in the expansion (4.1). Future work will compare these wave speeds to the exact ones computed in [17].

In Fig. 2 the curves representing these results are presented in the (b, c) plane.

Clearly, since c_1 and c_2 remain negative in the region of the (b, c) plane shown, with the exception of a very small b values, both solitary wave families correspond to leftward going waves in most of region of the (b, c) plane shown in this figure.

Also, note that both curves lie above the boundary curve parabola $c = -\frac{b^2}{4}$ of Fig. 1(a). These are the curves labeled C_2 and C_3 in that figure. Hence, the solitary waves which we have constructed here lie in Regions 2 and 4 of Fig. 1(a). Finding embedded solitary waves in Region 4 is particularly significant, since neither homoclinic orbits (corresponding to regular solitary waves of the original NLPDE) or families of homoclinics to small periodic solutions (corresponding to solitary waves with small tails for the original NLPDE) are widely known or discussed in the literature in that region of Fig. 1(a) [12]. Solitary waves in Region 1 are more widely known and have been reported in various models [9,12,18], including some created by a so-called orbit flip bifurcation which creates an infinite family of homoclinic orbits in this region. For our particular system (3.4), our results here reveal an infinite family of homoclinics to small periodic solutions corresponding to solitary waves with exponentially small tails as shown in [10] for the special parameter value $b = 1$, with embedded solitons for isolated parameter sets on the right halves of the c_1 and c_2 curves in Fig. 2.

Next, let us contrast the embedded solitary waves we have derived above with those derived by a very similar treatment in [10] using perturbations of a different family of unperturbed solutions given by (B.5) and only for the specific parameter value $b = 1$. The unique embedded solitary waves derived in [10] have wave speeds lying in the range $c \in \left(-\infty, \frac{1}{4}\right)$ with the parameter $b = 1$. Hence they lie along the lower half of the vertical line at $b = 1$ shown in red in Fig. 2. It is straightforward to check that this line starts on the curve C_2 in Fig. 1(a) and stretches straight up from there. Hence those embedded solitary waves in [10] lie along that vertical line at $b = 1$ in regions 3 or 4 of Fig. 1(a).

By contrast, the embedded solitary waves derived in this paper based on perturbations of a family of unperturbed solutions (B.1) (disjoint from those used in [10]) are clearly entirely different, and lie on the parameter curves c_1 and c_2 in Fig. 2 lying in regions 3 and 4 of Fig. 1(a).

6. Asymmetric nonlocal solitary waves

Symmetric nonlocal solutions have already been discussed in [11]. Hence, we next consider asymmetric nonlocal solitary waves. We start by revisiting the first-order perturbation solution v_1 in Eq. (B.6). In this general case, the v_1 solution is

$$v_1(\zeta) = v_{1s}(\zeta) + \gamma \Psi_2(\zeta), \quad (6.1)$$

where v_{1s} is the symmetric inhomogeneous solution studied in [11], Ψ_2 is the antisymmetric homogeneous solution given in (B.8), and γ is an arbitrary constant. This way, v_1 is now antisymmetric if $\gamma \neq 0$. For asymptotic behaviors of solution v_{1s} given by (4.2), R and ϕ are related through (4.4).

We calculate higher order corrections in the perturbation expansion (4.1) to determine if the asymmetric solution $v(\zeta)$ with v_1 given in (6.1) can exist. At order ε^2, the equation for v_2 is:

$$Lv_2 = W, \quad (6.2)$$

where

$$W = -\{a_1(v_0v_1'' + v_1v_0'') + (a_2 - a_1)v_0'v_1' + a_3v_0^2v_1 + 3v_1^2 + 10v_1v_1'' + 5v_1''^2 + 30v_0v_1^2\}. \quad (6.3)$$

For the solution v_2 to be bounded at infinity, the right hand side of Eq. (6.2) must be orthogonal to the localized homogeneous solution v_0'. Hence,

$$\langle W, v_0' \rangle = 0. \quad (6.4)$$

To calculate the inner product $\langle W, v_0' \rangle$, we must recall the form of operator L, which implies

$$\langle Lv_1, v_1' \rangle = \left[v_1''' v_1' + \frac{a_2}{2} v_1'^2 - \frac{1}{2} v_1''^2 - \frac{a_3}{2} v_1^2 \right]\Big|_{-\infty}^{\infty} - \int_{-\infty}^{\infty} \left(3v_1^2 + 5v_1'^2 + 10 v_1 v_1'' + 30 v_0 v_1^2 \right) v_0' \, d\zeta, \tag{6.5}$$

and recalling Eq. (B.6), we have

$$\langle Lv_1, v_1' \rangle = \int_{-\infty}^{\infty} \left[a_1 (v_0 v_1'' + v_0'' v_1) + (a_2 - a_1) v_0' v_1' + a_3 v_0^2 v_1 - 3(2a_1 - a_2) v_0'' v_1 \right] v_0' \, d\zeta. \tag{6.6}$$

When Eqs. (6.5) and (6.6) are equated, and v_1 in (6.1) and the asymptotic behaviors (4.2) and (B.10) of v_{1s} and Ψ_2 utilized, we find

$$\langle W, v_0' \rangle = \gamma \left[-c - p^2(-b + 3p^2) \right] R \cos(\phi - \phi_2) + 3(2a_1 - a_2) \int_{-\infty}^{\infty} v_0' v_0'' \Psi_2 \, d\zeta. \tag{6.7}$$

The integral above can be computed with the help of Mathematica, and the result is

$$\int_{-\infty}^{\infty} v_0' v_0'' \Psi_2 \, d\zeta = -\frac{p(k^2 + p^2)}{70} \Big[6120k^2 + p^4(-216 + 180b + 17p^2) + k^2 p^2 (972 - 810b + 3373p^2) - 4k^4 (54 - 45b + 7390p^2) \Big] \pi \operatorname{csch}\left(\frac{\pi p}{k} \right). \tag{6.8}$$

Next, substituting Eqs. (B.16), (4.4), and (6.8) into (6.7), yields

$$\langle W, v_0' \rangle = -\Bigg[\gamma(-c + bp^2 - 3p^4) R \cos(\phi - \phi_2) - \frac{3\gamma(2a_1 - a_2)}{70} p(k^2 + p^2) \Big\{ 6120k^6 + p^4(-216 + 180b + 17p^2) + k^2 p^2 (972 - 810b + 3373p^2) - 4k^4 (54 - 45b + 7390p^2) \Big\} \pi \operatorname{csch}\left(\frac{\pi p}{k} \right) \Bigg]. \tag{6.9}$$

Eq. (6.9) is an important intermediate result. We discuss its implications for the existence of asymmetric nonlocal solitary waves next.

6.0.1. For Hamiltonian perturbations, $a_2 = 2a_1$.

Under such perturbations, if condition (5.1) for localized solitary waves does not hold, $\langle W, v_{0z} \rangle = 0$ if either of two conditions are met:

$$\gamma = 0 \tag{6.10}$$

corresponding to symmetric nonlocal waves which have already been treated earlier;
OR

$$-c + bp^2 - 3p^4 = 0, \tag{6.11}$$

which, together with $c = bk^2 + k^4$ and $c = p^4 - bp^2$, result in wavespeeds $c = -p^4 = -b^2/4, p^2 = b/2$.
OR

$$R \cos(\phi - \phi_2) = -\frac{\langle G(v_0), \Psi_3 \rangle}{p(4p^2 - 1 + b)} = 0 \tag{6.12}$$

which corresponds to the localized embedded solitary wave families with:
a. $a_2 = -a_1, a_3 = a_1, p^2 = -k^2 = b/2$, and arbitrary wavespeed $c_{family} = -b^2/4$. However, this is inconsistent with the requirement $a_2 = 2a_1$ for Hamiltonian perturbations.
OR
b. the isolated embedded soliton families with p given by (5.4), and the wavespeeds in (5.6) with the additional requirement $a_2 = 2a_1$ for Hamiltonian perturbations.

6.0.2. For non-Hamiltonian perturbations, $a_2 \neq 2a_1$.

For non-Hamiltonian perturbations, if condition (5.1) for localized solitary waves does not hold, $\langle W, v_0' \rangle = 0$ if any of three conditions are met:

$$-c + bp^2 - 3p^4 = 0, \qquad p^2 = -k^2, \tag{6.13}$$

which imply

$$b = \frac{1}{2}, \qquad k^2 = -p^2 = -\frac{1}{4}, \qquad c_{AW} = -\frac{1}{16}, \tag{6.14}$$

with the subscript denoting asymmetric waves;
OR

$$-c + bp^2 - 3p^4 = 0, \qquad p = 0, \qquad k^2 = 0, or - b \tag{6.15}$$

which yields standing waves with wavespeed $c = 0$;
OR

$$-c + bp^2 - 3p^4 = 0, \quad \text{and} \quad \Big\{ 6120k^6 + p^4(-216 + 180b + 17p^2) + k^2 p^2 (972 - 810b + 3373p^2) - 4k^4 (54 - 45b + 7390p^2) \Big\} = 0 \tag{6.16}$$

Using $c = bk^2 + k^4 = p^4 - bp^2$, this yields the distinguished or isolated sets of b values and associated asymmetric wave speeds:

$$a. \quad c_{AW} = -0.0045177, b = -0.134398, \tag{6.17}$$

$$b. \quad c_{AW} = -2.4497, b = 2.40807, \tag{6.18}$$

AND

$$c. \quad c_{AW} = -34.0021, b = 11.6623. \tag{6.19}$$

7. Dynamics of ESs

In this section we follow the treatment in [10] to study the evolution of FKdV solitons under general perturbations. We apply dynamic soliton perturbation theory to Eq. (3.4), while heavily utilizing results from the previous sections.

When $\varepsilon = 0$, Eq. (3.4) is the integrable FKdV equation, which supports a family of solitons given by (2.2) and (B.1). These move at constant speed c and are stationary. When perturbations are imposed, that is, when $0 \neq \varepsilon \ll 1$, this velocity changes depending on the slow time scale $T = \varepsilon^2 t$. Moreover, energy radiation rises as well, and so it is appropriate to introduce the spatial coordinate

$$\zeta = x - \int_0^t c \, dT, \tag{7.1}$$

which moves with the soliton.

Then

$$v(x,t) = v\left(x - \int_0^t c \, dT \right) \equiv v(\zeta).$$

Considering this, Eq. (3.4) becomes,

$$v_t - cv' + 6vv' + bv''' + v' + 10vv''' + 20v'v'' + 30v^2 v' = \varepsilon F(v), \tag{7.2}$$

with the $'$ denoting a derivative with respect to ζ.

We propose a solution with the form

$$v(\zeta, t) = v_0(\zeta, T) + \varepsilon v_1(\zeta, t, T) + \varepsilon^2 v_2(\zeta, t, T) + \cdots. \tag{7.3}$$

Here, v_0 is given in Eq. (B.1) but because $c = c(T)$, we have $k = k(T)$, and v_0 depends on the slow time T as well.

At ϵ order, the following equation is obtained:

$$\frac{\partial v_1}{\partial t} = (Lv_1)' = G'(v_0) = F(v_0). \tag{7.4}$$

The nonhomogeneous term in (7.4) continuously excites the continuous wave (cw) tails that propagate into the far field. A significant observation is that these cw tails only appear ahead of the soliton, not behind

it. This is due to the fact that the group velocity of the cw waves in v_1 relative to the moving frame is positive for all $C > 0$. Consequently, for $t \gg 1$,

$$v_1(\zeta, t) \to \begin{cases} \tilde{R}\sin(p\zeta + \tilde{\phi}), & x \gg 1, \\ 0, & x \ll -1. \end{cases} \tag{7.5}$$

As t tends to infinity, the solution v_1 approaches a steady state with the asymptotic behavior described in (7.5). In this case, the time derivative in Eq. (7.4) can be neglected. Integrating once with respect to ζ, and utilizing the asymptotic behavior (7.5) of v_1 at negative infinity, we find that the steady-state solution satisfies (B.6) and the boundary condition (7.5).

Furthermore, by exploiting the self-adjoint property of L and using Eqs. (B.13) and (4.3), along with the asymptotic behaviors described in Eqs. (B.10), (B.11), and (7.5), the following results can be derived:

$$\langle G(v_0), \Psi_2\rangle = p(2p^2 - b)\tilde{R}\sin(\tilde{\phi} - \phi_2) = 0, \tag{7.6}$$

$$\langle G(v_0), \Psi_3\rangle = p(2p^2 - b)\tilde{R}\sin(\tilde{\phi} - \phi_3). \tag{7.7}$$

Therefore, the amplitude $\tilde{R}$ and phase $\tilde{\phi}$ can be determined as follows:

$$\tilde{R} = \frac{\langle G(v_0), \Psi_3\rangle}{p(2p^2 - b)}, \qquad \tilde{\phi} = \phi_2 \tag{7.8}$$

It is important to note that $\langle G(v_0), \Psi_3\rangle$ has been provided in Eq. (B.16). It should also be mentioned that the alternative solution to Eqs. (7.6)–(7.7) is $\tilde{\phi} = \phi_2 \pm \pi$, and $\tilde{R}$ is the negative of the expression given in (7.8). However, this solution leads to the same tail behavior (7.5) as (7.8), and therefore can be disregarded.

Eq. (7.9) represents another significant result of this article. Firstly, $\tilde{\phi} = \phi_2$ indicates that the phase of the cw tail ahead of the soliton is the same as the phase of the antisymmetric homogeneous solution at infinity. At this phase, $\tilde{R}$ is minimized, as can be observed by checking Eqs. (B.13) and (7.7). Hence, when perturbed, the soliton emits the minimal possible cw tail radiation [10]. Secondly, the tail amplitude $\tilde{R}$ of the one-sided nonlocal solitary wave is twice that of the symmetric nonlocal wave with the same phase, as verified in Eqs. (4.4) and (7.7).

The steady-state solution v_1 can be decomposed as follows:

$$v_1(\zeta) = v_{1s}(\zeta) + \frac{1}{2}\tilde{R}\Psi_2(\zeta), \tag{7.9}$$

where v_{1s} represents the symmetric component and exhibits the following asymptotic behavior:

$$v_{1s}(\zeta) \to \pm\frac{1}{2}\tilde{R}\sin(p\zeta \pm \Psi_2), \qquad \zeta \to \pm\infty. \tag{7.10}$$

Therefore, the tail amplitude $\tilde{R}$ of v_1 is twice that of the symmetric nonlocal wave v_{1s}.

With the first-order solution v_1 fully determined, we can proceed to order ϵ^2. The equation for v_2 is given by:

$$\frac{\partial v_2}{\partial t} + (Lv_2)' = W' - \frac{\partial v_0}{\partial T}, \tag{7.11}$$

where the expression for W is provided in Eq. (6.3). By using (7.11), it can be found that:

$$\frac{\partial\langle v_2, v_0\rangle}{\partial t} = \langle W' - \frac{\partial v_0}{\partial T}, v_0\rangle, \tag{7.12}$$

which implies that we must satisfy $\langle W_\zeta - v_{0T}, v_0\rangle = 0$ to suppress secular growth in v_2.

Using the above result, together with the relation $c = bk^2 + k^4$ yields

$$\frac{dc}{dT} = -\frac{2}{15k}(2k^2 + b)\langle W, v_0'\rangle \tag{7.13}$$

for the slow or long-time modulation of the wavespeed. The fixed points of this equation yield the possible solitary waves, both symmetric and asymmetric ones, and their stability allows us to deduce the stability of the corresponding wave solutions. We now proceed to employ (7.13) to investigate the dynamics of both the embedded solitons and non-local solitary waves of our system.

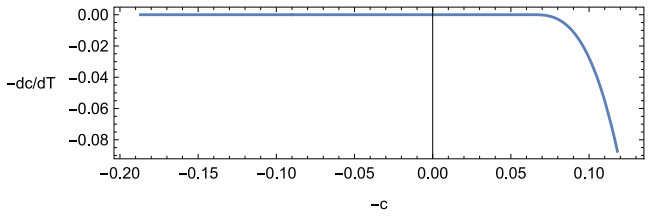

Fig. 3. Stability diagram for (7.14) and (6.13).

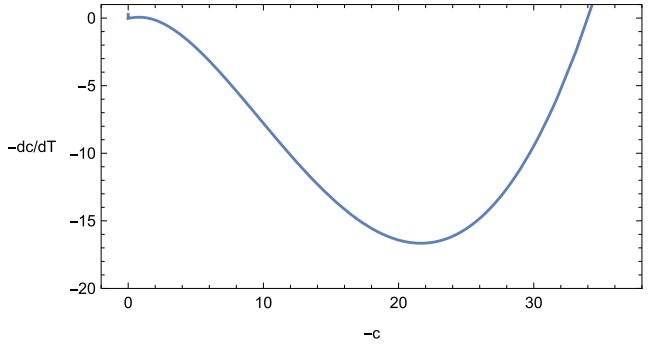

Fig. 4. Stability diagram for (6.17)–(6.19).

First, note that the pre-factor $(2k^2 + b)$ on the right hand side of (7.13) introduces an additional condition

$$2k^2 + b = 0, \tag{7.14}$$

for the existence of a solitary wave, over and above conditions (6.11), (6.13), (6.15), and (6.17)–(6.19) discussed at the end of the previous section. Of these, it is easy to check that conditions (7.14) and (6.13) are in fact equivalent. The plot of $\frac{dc}{dT}$ versus c is shown below for a representative parameter set $a_1 = 0.5, a_2 = 0.7, a_3 = 2, \gamma = 0.1$. (See Fig. 3.)

Clearly, the solitary wave with speed $c = -1/16$ is stable, with the flow returning any perturbation from that fixed point of the wavespeed back to the stationary value. *Note also that these stability results remain valid for the corresponding symmetric solitary waves with $\gamma = 0$ because the first term inside the square bracket in (6.9) is identically zero even with $\gamma \neq 0$ in this case.*

Next, for the cases in (6.17)–(6.19), the plot of $\frac{dc}{dT}$ versus c is shown below for the representative parameter set $a_1 = 0.5, a_2 = 0.7, a_3 = 2, \gamma = 0.1$. (See Fig. 4.)

So from the sign of $\frac{dc}{dT}$, the stationary points corresponding to solitary waves with wavespeeds $c = -34.0021, -1.4497$ and $c = -0.0045157$ are respectively unstable, stable, and unstable, with the flow below and above bringing it back to the stable point for the second case, and the flow below and above being away from the unstable fixed points in the first and third cases.

For the case (6.15), $\frac{dc}{dT} = 0$ for all b for the subcase $k = 0$, and hence this is a degenerate case. For the other subcases in (6.15) with $k^2 = -b$, it is straightforward to check that the fixed point of $\frac{dc}{dT}$ or solitary waves have wavespeed $c = 0$, or are stationary. Their stability around this stationary value is shown in Fig. 5.

Clearly, the flow is away from the stationary value or solitary wavespeed $c = 0$. Hence these solitary waves are unstable.

For the first Hamiltonian case (6.11) with the representative parameter set $a_1 = 0.5, a_2 = 0.7, a_3 = 2, \gamma = 0.1$, the wavespeeds may be real for a little perturbation δb around any value of b as shown in Fig. 6.

However, numerical evaluation yields imaginary values of $\frac{dc}{dT}$, hence the fixed point or possible solitary wave at $b = 0$, $\delta b = 0$ is not a valid one.

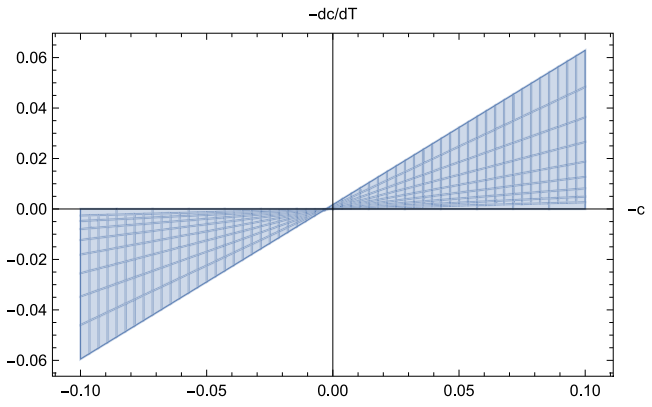

Fig. 5. Stability diagram for (6.15).

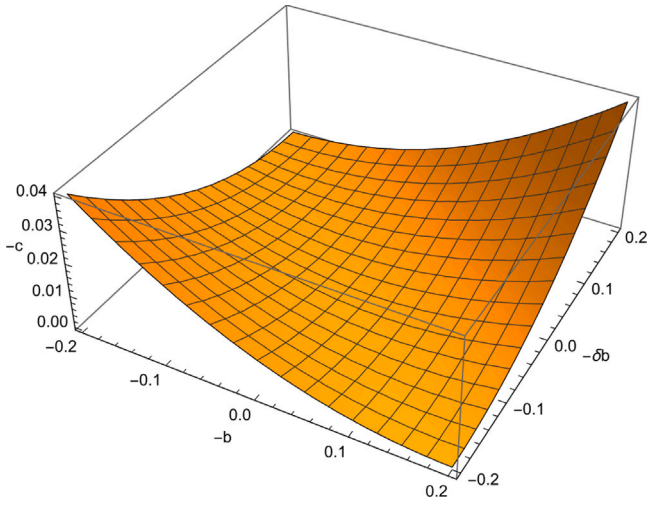

Fig. 6. Wavespeed for perturbation δb around various values of b for the case in (6.11).

Next, we consider the Hamiltonian case in (6.12). As discussed in the paragraph following (6.12), the only consistent possibilities are the isolated embedded soliton families with p given by (5.4), and the wavespeeds in (5.6) with the additional requirement $a_2 = 2a_1$ for Hamiltonian perturbations.

Considering these numerically for the representative parameter set $a_1 = 1.5, a_2 = 3, a_3 = 5, \gamma = 0.1$, and the first wavespeed $c_1 = \frac{3}{446}b(6 - 5b) + \frac{(9(6-5b)^2)}{198916}$ in (5.6), $\frac{dc}{dT}$ takes imaginary values for small deviations around its fixed point or possible solitary wave at $b = 2.92917$. Hence this is not a genuine possibility for a solitary wave solution. However, for the second wavespeed $c_2 = \frac{1}{462}b(18 + 23\beta) + \frac{(18-23b)^2}{213444}$ in (5.6), $\frac{dc}{dT}$ has zeros, corresponding to possible solitary waves, at various values, including $b = -0.136276, -0.463727, -1.13942, \ldots$. The corresponding stability diagram is shown in Fig. 7.

Clearly, stability switches in this case, with solitary waves at any root $c = c_i$ of $\frac{dc}{dT}$ being stable(unstable) if $\frac{dc}{dT} > 0$ just below(above) $c = c_i$, and $\frac{dc}{dT} < 0$ just above(below) it.

Finally, we briefly explicitly discuss the stability and dynamics of the three families of localized embedded solitary waves discussed in the paragraphs following (5.2). Asymmetric solutions with $\gamma \neq 0$ may exist for several cases. However, only two cases of non-trivial fixed points of (7.13), or solitary waves, need to be discussed separately.

The first is the same as those in (6.15) and (6.13) which have already been considered earlier in detail for both symmetric ($\gamma = 0$) and

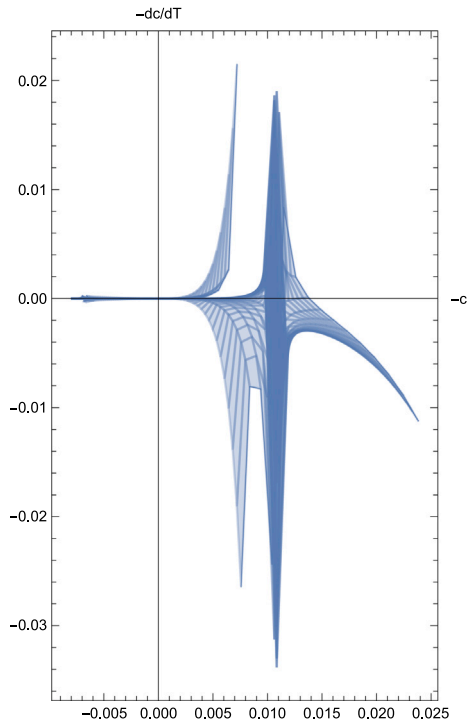

Fig. 7. Stability diagram for (6.11) and the second wavespeed in (5.6).

asymmetric ($\gamma \neq 0$) localized embedded solitary waves. The second non-trivial fixed-point of (7.13), or solitary wave, corresponds to $p^2 = -k^2$. In this second case, this fixed point or the corresponding solitary wave may be either stable or unstable depending not just on b, but also on the asymmetry parameter γ as well as a_1 and a_2. Hence, stability needs to be worked out on a case by case basis for each set of values of these four parameters.

In the next section we change gears and employ infinite series to compute homoclinic orbits of the traveling wave ODE (2.3) corresponding to traveling pulse solutions of the FKdV equation.

8. Analytic and numerical regular pulse solutions

In this Section we shall look for pulse solutions of Eq. (1.3). To this aim we shall compute Shil'nikov-type homoclinic orbits at the origin of the corresponding traveling wave equation (2.3), as given below:

$$v(\zeta) = \begin{cases} v^+(\zeta) = \sum_{k=1}^{\infty} a_k e^{k\alpha\zeta} + c.c., & \text{if } \zeta > 0 \\ v_0, & \text{if } \zeta = 0 \\ v^-(\zeta) = \sum_{k=1}^{\infty} b_k e^{k\beta\zeta} + c.c.. & \text{if } \zeta < 0 \end{cases} \tag{8.1}$$

The solution $v(\zeta)$ in (8.1) should tend to zero when $\zeta \to \pm\infty$, therefore α and β should be such that the following conditions hold:

$$\Re\mathrm{e}(\alpha) < 0 \qquad \text{and} \qquad \Re\mathrm{e}(\beta) > 0. \tag{8.2}$$

Moreover, the value $v(0) = v_0$ will be the maximum of the solitary solution. The coefficients a_k and b_k, with $k \geq 1$ are arbitrary coefficients to be determined.

We firstly determine the solution $v^+(\zeta)$ for $\zeta > 0$. Once substituted $v^+(\zeta)$, as defined in (8.1), into Eq. (2.3), we obtain:

$$\sum_{k=1}^{\infty} \left(a(k\alpha)^4 + b(k\alpha)^2 - c\right) a_k e^{k\alpha\zeta} = F_1 + F_2, \tag{8.3}$$

where:

$$F_1 = \begin{cases} 0 & \text{if } k = 1 \\ \sum_{k=2}^{\infty} F_1^{(k)} & \text{if } k > 1 \end{cases}, \qquad F_2 = \begin{cases} 0 & \text{if } k = 1, 2 \\ \sum_{k=3}^{\infty} F_2^{(k)} & \text{if } k > 2 \end{cases}, \tag{8.4}$$

with:

$$F_1^{(k)} = \sum_{i=1}^{k-1} \left(-\alpha_3 (k-i)^2 \alpha^2 + \frac{1}{2}(\alpha_3 - \alpha_4) i\alpha^2 - \frac{\alpha_1}{2} \right) a_{k-i} a_i e^{k\alpha\zeta}, \tag{8.5}$$

$$F_2^{(k)} = \sum_{j=2}^{k-1} \sum_{l=1}^{j-1} -\frac{\alpha_2}{3} a_{k-j} a_{j-l} a_l e^{k\alpha\zeta}. \tag{8.6}$$

We now compare in (8.3) the coefficients of $e^{k\alpha z}$ for each k, so that a sequence of equations, in the unknowns α and a_k, is obtained.

For $k = 1$ we have:

$$\left(a\alpha^4 + b\alpha^2 - c \right) a_1 = 0. \tag{8.7}$$

Assuming $a_1 \neq 0$, Eq. (8.7) is satisfied when α is a solution of the characteristic equation (2.8). We look for a root of Eq. (2.8) which satisfies condition in (8.2). As reviewed in Appendix A, in Region 1 depicted in Fig. 1, the solutions of the characteristic equation (2.8) are of the form $\pm\lambda \pm i\omega$. We thus select the system parameters in such Region 1, so that condition (8.2) holds choosing the following solution:

$$\alpha = -\lambda + i\omega. \tag{8.8}$$

The coefficient a_1 is still undetermined at this level.

For $k > 1$, we obtain:

$$p(k\alpha) a_k = F_1^{(k)} + F_2^{(k)}, \tag{8.9}$$

where:

$$p(k\alpha) = a(k\alpha)^4 + b(k\alpha)^2 - c. \tag{8.10}$$

Notice that $p(k\alpha) \neq 0$ for $k > 1$.

For $k = 2$, Eq. (8.9) reads:

$$p(2\alpha) a_2 = -\frac{1}{2} \left((\alpha_3 + \alpha_4)\alpha^2 + \alpha_1 \right) a_1^2, \tag{8.11}$$

where $p(k\alpha)$ is defined in (8.10).

Therefore, a_2 can be given in terms of a_1 in the form:

$$a_2 = \varphi_2 a_1^2 \tag{8.12}$$

where:

$$\varphi_2 = -\frac{(\alpha_3 + \alpha_4)\alpha^2 + \alpha_1}{2p(2\alpha)} \tag{8.13}$$

is a known coefficient, computed in terms of the parameters of Eq. (2.3) and the exponent α obtained at order $k = 1$.

Let us iterate the analysis computing Eq. (8.9) for $k = 3$:

$$p(3\alpha) a_3 = -\frac{1}{2} \left((7\alpha_3 + 3\alpha_4)\alpha^2 + 2\alpha_1 \right) a_1 a_2 - \frac{\alpha_2}{3} a_1^3. \tag{8.14}$$

Taking into account the expression for a_2 in terms of a_1 obtained in (8.12), Eq. (8.14) gives a_3 in terms of a_1:

$$a_3 = \varphi_3 a_1^3, \quad \text{with} \quad \varphi_3 = -\frac{3\left((7\alpha_3 + 3\alpha_4)\alpha^2 + 2\alpha_1 \right)\varphi_2 + 2\alpha_2}{6p(2\alpha)p(3\alpha)}. \tag{8.15}$$

In general, for $k > 3$, the series coefficients a_k have the following expression:

$$a_k = \frac{F_1^{(k)} + F_2^{(k)}}{p(k\alpha)}, \tag{8.16}$$

and $F_1^{(k)}$ and $F_2^{(k)}$ can be inductively obtained as the product of a_1^k with a known quantity, computed in terms of the exponent α and the parameters of Eq. (2.3), so that the coefficients a_k have the following expression for all $k > 1$:

$$a_k = \varphi_k a_1^k. \tag{8.17}$$

Using the solution in (8.8) for α and the coefficients a_k, with $k > 1$, given in (8.17), then the first part $v^+(\zeta)$ of the homoclinic orbit (8.1) has been computed in terms of the coefficient a_1:

$$v^+(\zeta) = a_1 e^{\alpha\zeta} + \sum_{k=2}^{\infty} \varphi_k a_1^k e^{k\alpha\zeta} + c.c.. \tag{8.18}$$

Proceeding as above to compute the solution $v^-(\zeta)$ in (8.1), we get:

$$\beta = \lambda + i\omega \qquad \text{and} \qquad v^-(\zeta) = b_1 e^{\beta\zeta} + \sum_{k=2}^{\infty} \psi_k b_1^k e^{k\beta\zeta} + c.c.. \tag{8.19}$$

We recall that Eq. (2.3) is reversible, therefore the solution $v(\zeta)$ in (8.1) should be symmetric with respect to $\zeta = 0$. Therefore, from expressions (8.18) and (8.19), it follows that:

$$\varphi_k = \psi_k. \tag{8.20}$$

Since the solution in (8.1) should be continuous in $\zeta = 0$, we impose:

$$v^+(0) = v_0 = v^-(0), \tag{8.21}$$

so that it is sufficient to choose $a_1 = b_1$, with a_1 satisfying:

$$a_1 + \sum_{k=2}^{\infty} \phi_k a_1^k + c.c. = v_0. \tag{8.22}$$

In order to determine a_1, we truncate the sum in (8.22) at some $k = M$, so that a_1 is a solution of $M-$degree polynomial. This truncation can be done because the series in (8.1) converges. In fact, following the same lines as in [19], it is straightforward to obtain the following bound for the series coefficients:

$$|a_k| < l(\alpha_3, \alpha_4, \xi)^{-(k+1)} |a_1|^k, \tag{8.23}$$

where the constant $l(\alpha_3, \alpha_4, \xi)$ depends on the parameters α_3 and α_4 of Eq. (2.3) and also on the Euler's constant ξ. The bound given in (8.23) validates the steep fall-off in the magnitude of the late terms of the series solution (8.1).

We thus numerically compute the solution of the truncated $M-$degree polynomial corresponding to (8.22). This solution is not unique, therefore also the homoclinic orbit in (8.1) is not unique.

8.1. Numerical investigation of regular pulse solutions

We now test the above analytical results specifying the parameters of the traveling wave equation corresponding to the FKdV equation (2.3) in some cases already known in literature and for which traveling wave solutions have been already investigated.

Choosing the parameters as in the numerical tests given below, we obtain that the bound in (8.23) can be evaluated as:

$$|a_k| < 10^{-(k+1)} |a_1|^k, \quad k > 4. \tag{8.24}$$

Therefore, the coefficients $|a_k|$, with $k > 4$, can be bounded by some constant $L > 0$. The series of absolute values associated to $v^+(\zeta)$ and $v^-(\zeta)$, given in (8.1), can be bounded by L times a convergent exponential (geometric) series, so that the series solution (8.1) is absolutely convergent, and hence convergent due to the Comparison Test.

We underline that the later coefficients, computed in the following numerical tests drop off sharply in magnitude. In particular, we have observed that the coefficients φ_k and ψ_k, with $k > 20$, are order 10^{-16}.

Numerical test 1 We firstly re-obtain the regular solitons found in [9]. The authors look for stationary solutions of the FKdV in the form of traveling waves for the following fourth-order ODE (see the Eq. (13) in [20]):

$$Bv'''' + v'' - Vv = -\frac{v^2}{2} - \frac{s}{3} v^3 - \frac{G_1}{2} v v'' + \frac{1}{2}(3G_1 - G_2) v'^2, \tag{8.25}$$

where $' = \frac{d}{d\zeta}$. Notice that Eq. (8.25) has exactly the same terms as in (2.3) with:

$$a = B, \quad b = 1, \quad c = V, \quad \alpha_1 = 1, \quad \alpha_2 = s, \quad \alpha_3 = G_1, \quad \alpha_4 = G_2. \tag{8.26}$$

The bifurcation diagram is as in Fig. 1(b) considered in the plane (B, V). We choose the parameters as in Fig. 9(a) of the paper [20], where the case of negative cubic term $s = -1$ is investigated. With

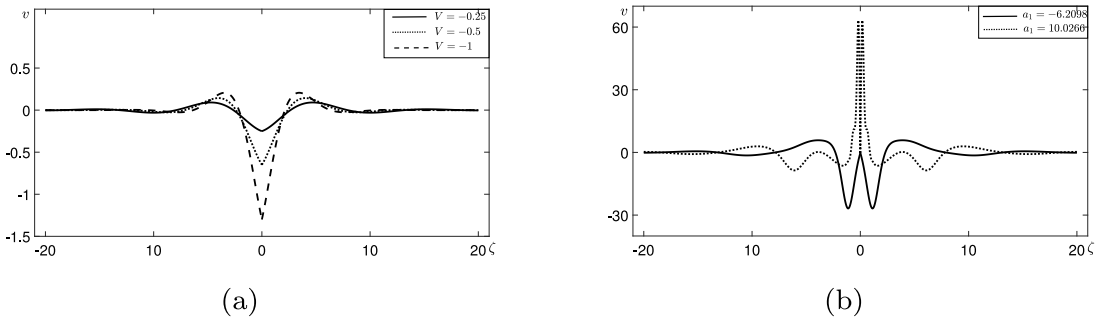

Fig. 8. Series solutions (8.1) for the traveling wave equation (8.25). The parameters $B = 8/5$, $G_1 = G_2 = 0$ and $s = -1$ are chosen as in Fig. 9(a) of the paper [20]. (a) For $V = -0.25$, we have $\alpha = -0.2035 \pm i0.5949$, we choose $v_0 = -0.25$ and truncate the continuity condition (8.22) at $M = 20$. The solid line corresponds to the solution (8.1) choosing $a_1 = -0.125$ which solves the truncated equation (8.22). For $V = -0.5$, we have $\alpha = -0.3511 \pm i0.6601$, we choose $v_0 = -0.65$ and truncate the continuity condition (8.22) at $M = 20$. The dotted line corresponds to the solution (8.1) choosing $a_1 = -0.3297$ which solves the truncated equation (8.22). For $V = -1$, we have $\alpha = -0.4889 \pm i0.7427$, we choose $v_0 = -1.3$ and truncate the continuity condition (8.22) at $M = 20$. The dashed line corresponds to the solution (8.1) choosing $a_1 = -0.6631$ which solves the truncated equation (8.22).(b) The series solution (8.1) for $V = -0.25$ choosing other values of a_1 which satisfy the continuity condition (8.22).

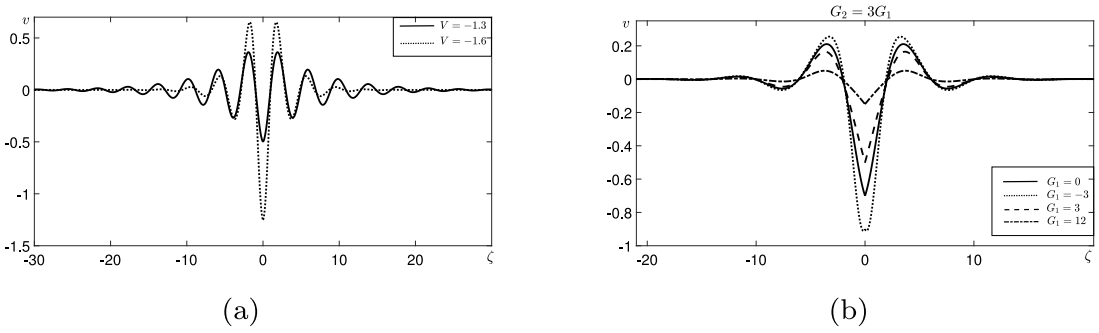

Fig. 9. Series solutions (8.1) for the traveling wave equation (8.25). (a) The parameters $B = 1/5$, $G_1 = G_2 = 0$ and $s = -1$ are chosen as in Fig. 10(a) of the paper [20]. For $V = -1.3$, we choose $v_0 = -0.5$ and truncate the continuity condition (8.22) at $M = 20$. The solid line corresponds to the solution (8.1) choosing $a_1 = -0.2477$ which solves the truncated equation (8.22). For $V = -1.6$, we choose $v_0 = -1.25$ and truncate the continuity condition (8.22) at $M = 20$. The dotted line corresponds to the solution (8.1) choosing $a_1 = -0.6617$ which solves the truncated equation (8.22). (b) The parameters $B = 1$, $V = -0.5$, $G_2 = 3G_1$ and $s = -1$ are chosen as in Fig. 13(a) of the paper [20]. For $G_1 = 0$, we choose $v_0 = -0.7$ and truncate the continuity condition (8.22) at $M = 20$. The solid line corresponds to the solution (8.1) choosing $a_1 = -0.3526$ which solves the truncated equation (8.22). For $G_1 = -3$, we choose $v_0 = -0.8$ and truncate the continuity condition (8.22) at $M = 20$. The dotted line corresponds to the solution (8.1) choosing $a_1 = -0.4104$ which solves the truncated equation (8.22). For $G_1 = 3$, we choose $v_0 = -0.5$ and truncate the continuity condition (8.22) at $M = 20$. The dashed line corresponds to the solution (8.1) choosing $a_1 = -0.28$ which solves the truncated equation (8.22). For $G_1 = 12$, we choose $v_0 = -0.15$ and truncate the continuity condition (8.22) at $M = 20$. The solid line corresponds to the solution (8.1) choosing $a_1 = -0.0863$ which solves the truncated equation (8.22).

$B = 8/5$ and $G_1 = G_2 = 0$, we should choose $V < -1/(4B) = -0.1563$ in such a way to consider a parameter set in Region 1 (below the curve C_2 in Fig. 1(b)). The value $V = -0.25$, chosen in the numerical simulation in Fig. 9(a) of [20], satisfies this condition, in fact the solution of the characteristic equation (2.8) are $\pm 0.2035 \pm i0.5949$. We thus choose $\alpha = -0.2035 \pm i0.5949$, fix $v_0 = -0.25$, truncate the series solution at $M = 20$ and solve Eq. (8.22), which has four real solutions $a_1 = -0.125$ or $a_1 = -6.2098$ or $a_1 = 10.0266$ or $a_1 = -14.9554$. Choosing $a_1 = -0.125$, we draw the series solution as the solid line in Fig. 8(a) which reproduce the regular soliton obtained in Fig. 9(a) of the paper [20]. The solutions corresponding to the other values of a_1 which satisfy the truncated continuity condition (8.22) are the homoclinic orbits drawn in Fig. 8(b). We also reconstruct, using the series solution (8.1), the regular solitons for $V = -0.5$ and $V = -1$ (see Fig. 8(a)).

In the following Fig. 9(a) we choose the parameters as in Fig. 10(a) of the paper [20]. With $B = 1/5$, the suitable values of V, so that the convergent series solution approach works, should be chosen less than $1/(4B) = -1.25$ (in Region 1 below the curve C_2 in Fig. 8(b)). Both the values $V = -1.3$ and $V = -1.6$ chosen in Fig. 10(a) of [20] satisfy this condition, therefore we compute the series solutions shown in Fig. 9(a) corresponding to the regular solitons obtained in Fig. 10(a) of the paper [20] (see details into the caption of Fig. 9(a)).

Finally, we investigate the regular solitons arising for values of G_1 and G_2 different form zero, choosing the parameters as in Fig. 13(a) of the paper [20]. Since $B = 1$, the value of V should be chosen less than $-1/(4B) = -0.25$ so that the eigenvalues of the characteristic equation (2.8) are as in Region 1 below the curve C_2 in Fig. 8(b). In Fig. 13(a) of [20] the value of the parameter V is -0.5, therefore the convergent series solution (8.1) can be computed. The resulting regular soliton is given in Fig. 9(b) and the details are all reported into the caption of the same figure.

Numerical test 2 Let us now consider the following equation:

$$\frac{2}{15}v'''' + bv'' - cv = -\frac{3}{2}v^2 - \mu v v'' + \frac{3}{2}\mu v'^2, \tag{8.27}$$

which has been investigated in [12,18]. The Eq. (8.27) corresponds to (2.3) with:

$$a = \frac{2}{15}, \qquad \alpha_1 = 3, \qquad \alpha_2 = 0, \qquad \alpha_3 = \mu, \qquad \alpha_4 = 4\mu. \tag{8.28}$$

The bifurcation diagram of Eq. (8.27) is qualitatively equal to that one drawn in Fig. 1(a), with a fixed positive (in this case the concave parabola has the equation $c = -\frac{15}{8}b^2$). The homoclinic orbits as in (8.1) can be therefore computed in Region 1 (below the parabola) where the origin is a saddle-focus. In Fig. 10(a) we fix $b = -4/3$ and $c = -3.34$ or $c = -3.5$ so that the solutions of the characteristic equation (2.8) are as in Region 1 (below the curve C_2), finding the two regular solitons shown in Fig. 10(a). In Fig. 10(b) we show the regular solitons arising once we choose the parameters so that the eigenvalues are as in Region 1, but below the curve C_3.

Numerical test 3 We consider the traveling wave equation corresponding to the FKdV as given in [10]:

$$v'''' + v'' - cv = -3v^2 - c_3\frac{v^3}{3} - c_1 v v'' + \frac{(c_1 - c_2)}{2}v'^2. \tag{8.29}$$

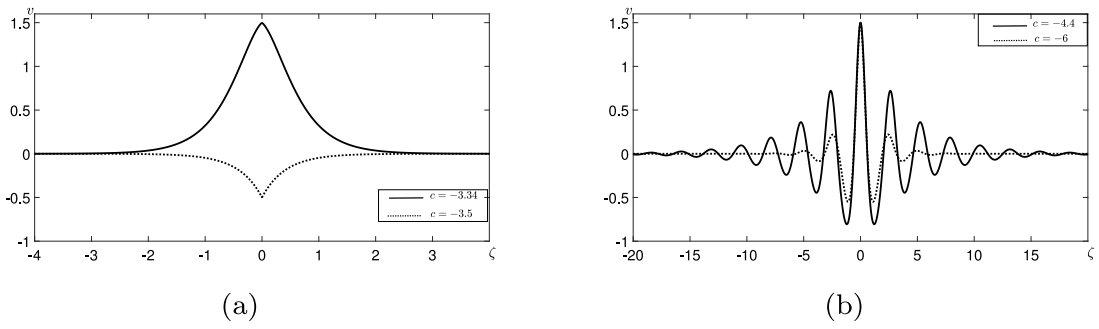

Fig. 10. Series solutions (8.1) for the traveling wave equation (8.27). (a) The parameters are chosen as $\mu = 1$, $b = -\frac{4}{3}$. For $c = -3.34$, we choose $v_0 = 1.5$ and truncate the continuity condition (8.22) at $M = 20$. The solid line corresponds to the solution (8.1) choosing $a_1 = 1.6375$ which solves the truncated equation (8.22). For $c = -3.5$, we choose $v_0 = -0.5$ and truncate the continuity condition (8.22) at $M = 20$. The dotted line corresponds to the solution (8.1) choosing $a_1 = -0.2280$ which solves the truncated equation (8.22). (b) The parameters are chosen as $\mu = 1$, $b = 1.5$. For $c = -4.44$, we choose $v_0 = 1.5$ and truncate the continuity condition (8.22) at $M = 20$. The solid line corresponds to the solution (8.1) choosing $a_1 = 0.6216$ which solves the truncated equation (8.22). For $c = -6$, we choose $v_0 = -0.5$ and truncate the continuity condition (8.22) at $M = 20$. The dotted line corresponds to the solution (8.1) choosing $a_1 = 0.6734$ which solves the truncated equation (8.22).

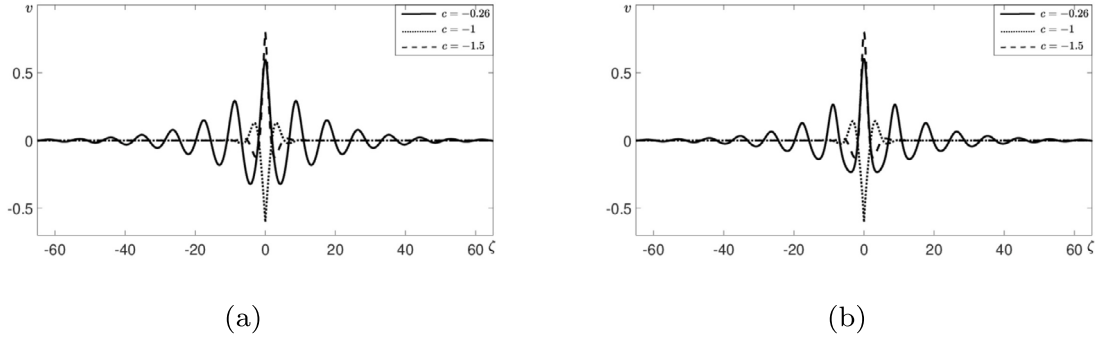

Fig. 11. Series solutions (8.1) for the traveling wave equation (8.29). (a) The parameters are chosen as $(c_1, c_2, c_3) = \left(\frac{110}{19}, \frac{230}{19}, -\frac{60}{19}\right)$. For $c = -0.26$, we choose $v_0 = 0.6$ and truncate the continuity condition (8.22) at $M = 20$. The solid line corresponds to the solution (8.1) choosing $a_1 = 0.2457$ which solves the truncated equation (8.22). For $c = -1$, we choose $v_0 = -0.6$ and truncate the continuity condition (8.22) at $M = 20$. The dotted line corresponds to the solution (8.1) choosing $a_1 = -0.3446$ which solves the truncated equation (8.22). For $c = -1.5$, we choose $v_0 = 0.8$ and truncate the continuity condition (8.22) at $M = 20$. The dotted line corresponds to the solution (8.1) choosing $a_1 = 0.3730$ which solves the truncated equation (8.22).(b) The parameters are chosen as $(c_1, c_2, c_3) = (10, 20, 30)$. For $c = -0.26$, we choose $v_0 = 0.6$ and truncate the continuity condition (8.22) at $M = 20$. The solid line corresponds to the solution (8.1) choosing $a_1 = 0.1996$ which solves the truncated equation (8.22). For $c = -1$, we choose $v_0 = -0.6$ and truncate the continuity condition (8.22) at $M = 20$. The dotted line corresponds to the solution (8.1) choosing $a_1 = -0.3862$ which solves the truncated equation (8.22). For $c = -1.5$, we choose $v_0 = 0.8$ and truncate the continuity condition (8.22) at $M = 20$. The dotted line corresponds to the solution (8.1) choosing $a_1 = 0.3733$ which solves the truncated equation (8.22).

This equation belongs to the class of Eq. (2.3) with:

$$a = 1, \qquad b = 1, \qquad \alpha_1 = 6, \qquad \alpha_2 = c_3, \qquad \alpha_3 = c_1, \qquad \alpha_4 = c_2. \tag{8.30}$$

The bifurcation diagram of Eq. (8.29) is qualitatively as in Fig. 1(a), with also $b = 1$. We therefore compute series solution (8.1) for homoclinic orbits in Region 1. In Fig. 11(a) we choose the parameters so that Eq. (8.29) describes irrotational gravity waves, i.e. $(c_1, c_2, c_3) = \left(\frac{110}{19}, \frac{230}{19}, -\frac{60}{19}\right)$.

In Fig. 11(b) we choose the parameters so that Eq. (8.29) describes the KdV hierarchy, i.e. $(c_1, c_2, c_3) = (10, 20, 30)$.

In Fig. 12(a) we choose the parameters so that Eq. (8.29) describes the Sawada–Kotera equation, i.e. $(c_1, c_2, c_3) = (15, 15, 45)$.

In Fig. 12(b) we compare the series solution of Eq. (8.29) obtained in the three parameter sets corresponding to the irrotational gravity waves (solid line), the KdV hierarchy (dotted line) and the Sawada–Kotera equation (dashed line) for the same values of c and v_0.

9. Summary

In this paper, we have significantly generalized the results of [11] to the case of asymmetric nonlocal solitary waves. In addition, the dynamics and stability of both symmetric and asymmetric embedded solitons were treated in detail. Note that asymmetric solitary waves were not considered at all in [11]. Although [11] considered symmetric embedded solitary waves, it did not consider their stability. Moreover, the paper derives other novel families of regular solitary waves using multi-infinite series solutions.

CRediT authorship contribution statement

S. Roy Choudhury: Conceptualization, Data curation, Formal analysis, Investigation, Methodology, Supervision, Validation, Writing – original draft, Writing – review & editing. **Gaetana Gambino:** Conceptualization, Data curation, Formal analysis, Investigation, Methodology, Supervision, Validation, Writing – original draft, Writing – review & editing. **Ranses Alfonso Rodriguez:** Conceptualization, Data curation, Formal analysis, Investigation, Methodology, Supervision, Validation, Writing – original draft, Writing – review & editing.

Declaration of competing interest

The authors declare that they have no known competing financial interests or personal relationships that could have appeared to influence the work reported in this paper.

Data availability

No data was used for the research described in the article.

Acknowledgments

The author GG acknowledges the financial support of the MUR-PRIN2017 grant (project no. 2017YBKNCE), the GNFM-INdAM and the FFR2022-FFR2023 grant of the University of Palermo, Italy.

Appendix A. Solitary waves and local bifurcations

Fig. 1 shows the regions of the parameters (in particular, Fig. 1(a) in the plane (b, c) and Fig. 1(b) in the plane (a, c)) where the eigenvalues of the characteristic equation (2.8) have different structure. These regions are labeled 1−4. While defining the structure of the orbits homoclinic to the fixed point of (2.3), we review the boundary curves of these regions and their neighborhoods, marked C_0-C_3, and the possible occurrence and multiplicities of homoclinic orbits of (2.3), which correspond to pulse solitary waves of Eq. (1.3) in the regions 1 through 4.

Near C_0: The eigenvalue structure on this curve is $\lambda_{1-4} = 0, 0, \pm i\sqrt{-\frac{b}{a}}$ (see $(ii.1)$ in Section 3), and it can be shown by analysis of a four-dimensional normal form [21] that on the side of C_0 corresponding to region 3 in Fig. 1 there is a sech^2 homoclinic orbit.

However, in region 1, where the eigenvalue structure is that of a saddle-center, the fixed point (2.5) is non-hyperbolic. It may be proved [22,23] that there are classes of orbits in region 1 which are homoclinic to periodic orbits as $\zeta \to \pm\infty$. These are so-called delocalized solitary waves [13]. Depending on the form of the nonlinear terms of the equation, this family of periodic orbits has amplitudes varying from zero to a size of order $\varepsilon^{\frac{1}{2}}$. Also, on isolated curves in region 3, the amplitude of these periodic solutions as ζ goes to zero, thus yielding truly localized solitary waves. These are known as embedded solitons [24] and will be investigated for our system (3.4) in Section 5.

Near C_1: On this curve the eigenvalues have the structure given in $(ii.2)$ of Section 3, i.e. $\lambda_{1-4} = 0, 0, \pm\sqrt{-\frac{b}{a}}$. C_1 and its vicinity have been considered via reversible systems theory in [21,25]. In this region, a standard analysis yields the normal form on the center manifold

$$\dot{x}_1 = x_2,$$
$$\dot{x}_2 = \mathrm{sign}(\mu)x_1 - \frac{3}{2}x_1^2,$$

where μ is an unfolding parameter [21]. For $\mu > 0$, it yields a unique, symmetric homoclinic solution

$$x_1(t) = \mathrm{sech}^2\,\frac{t}{2}$$

in the vicinity of C_1. One may also show persistence of this homoclinic solution in the original system (2.7) for $\mu > 0$ [21].

Near C_2: In this region, where $\lambda_{1-4} = \pm i\sqrt{-\frac{b}{2a}}, \pm i\sqrt{-\frac{b}{2a}}$ (see $(iii.1)$ in Section 3), derivation and analysis of a complicated normal form [26,27] shows the possible occurrence of so-called 'envelope' homoclinic solutions of the form $\mathrm{sech}\, kte^{i\gamma\theta}$ (and with oscillating tails) in the so-called 'subcritical' form. However, occurrence or persistence of these solutions in the full nonlinear system (1.3) is a non-trivial issue (and each system must be analyzed separately [27,28]). The persistence in (1.3) is considered in various ways in [27–29]. This is relatively straightforward for solutions having "one hump or peak". The open problem is for non-symmetric solutions.

Near C_3: There is no small-amplitude bifurcation on this curve, on which $\lambda_{1-4} = \pm\sqrt{-\frac{b}{2a}}, \pm\sqrt{-\frac{b}{2a}}$ (see $(iii.2)$ in Section 3) and the fixed point (2.7) remains hyperbolic. However, there is a bifurcation across it causing the creation of an infinite multiplicity of homoclinic orbits.

Next, we look at the each of the regions 1–4 in Fig. 1 to discuss the possible occurrence and multiplicity of homoclinic orbits in each.

Region 1: The generic situation in this region has already been considered in the discussion above pertaining to the region near curve C_1. As mentioned there, the structure and multiplicity of the delocalized solitons in Region 1, as well as the existence of embedded solitons on isolated curves, will be investigated for Eq. (3.4) in Section 5.

Region 2: In this region the eigenvalues are of the type $\lambda_{1-4} = \pm\lambda_1, \pm\lambda_2$ and the fixed point (2.5) is a hyperbolic saddle point. Thus, there is no 'a priori' reason for multiplicity of homoclinic orbits in this region. However, depending on the actual form of the nonlinear term, a symmetric homoclinic orbit to (1.3) may exist (see [26,27]). Also, depending on further conditions [28, 29], a further 'orbit-flip' bifurcation may cause complex dynamics in its neighborhood. These issues will need further investigation to establish possible existence of solitary wave solutions of (1.3) in this region.

Region 3: In this region the structure of the eigenvalues is $\lambda_{1-4} = \pm\lambda, \pm i\omega$ and the fixed point (2.5) is a saddle-focus. Using a Shil'nikov type analysis, one may show [30,31] for general reversible systems such as (1.3) that the existence of one symmetric homoclinic orbit implies the existence of an infinity of others. Hence, we expect our system to admit an infinity of such symmetric N-pulses for each $N > 1$. Here, a symmetric N-pulse oscillates N times in phase-space for $\zeta \in (-\infty, \infty)$ (or, more technically, crosses a transversal section to the primary symmetric 1 pulse N times). In the context of Eq. (1.3), these would be N-peaked solitary waves, and we expect an infinite

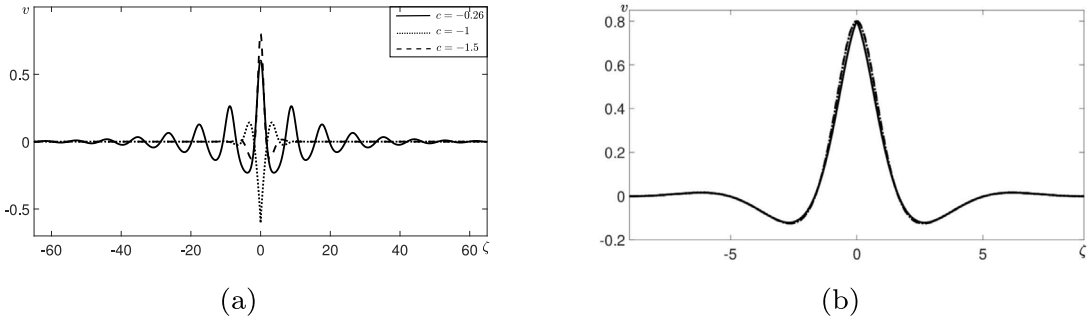

Fig. 12. Series solutions (8.1) for the traveling wave equation (8.29). (a) The parameters are chosen as $(c_1, c_2, c_3) = (15, 15, 45)$. For $c = -0.26$, we choose $v_0 = 0.6$ and truncate the continuity condition (8.22) at $M = 20$. The solid line corresponds to the solution (8.1) choosing $a_1 = 0.1980$ which solves the truncated equation (8.22). For $c = -1$, we choose $v_0 = -0.6$ and truncate the continuity condition (8.22) at $M = 20$. The dotted line corresponds to the solution (8.1) choosing $a_1 = -0.3869$ which solves the truncated equation (8.22). For $c = -1.5$, we choose $v_0 = 0.8$ and truncate the continuity condition (8.22) at $M = 20$. The dotted line corresponds to the solution (8.1) choosing $a_1 = 0.3757$ which solves the truncated equation (8.22).(b) Comparison between the series solutions of Eq. (8.29) for $c = -1.5$ and $v_0 = 0.8$: the solid line is the solution of (8.29) with $(c_1, c_2, c_3) = \left(\frac{110}{19}, \frac{230}{19}, -\frac{60}{19}\right)$, the dotted line is the solution of (8.29) with $(c_1, c_2, c_3) = (10, 20, 30)$ and the dashed line is the solution of (8.29) with $(c_1, c_2, c_3) = (15, 15, 45)$.

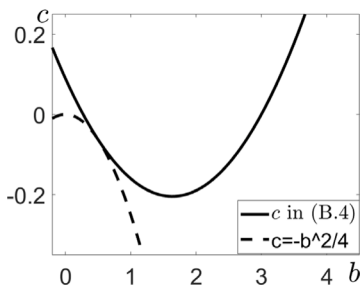

Fig. B.13. The mutual position of the curves $c = -\frac{b^2}{4}$, representing the two branches C_2 and C_3 in Fig. 1(a), and c as given in (B.4).

family for all $N > 1$ once chosen the parameters a, b and c in Region 1 of Fig. 1.

Region 4: In this region, the structure of the eigenvalues is $\lambda_{1-4} = \pm i\omega_1, \pm i\omega_2$ and (2.5) is a focus. No homoclinic orbits are known to exist in general here, although complex dynamics may occur [30,31]. Special results exist for $\omega_1 \approx \omega_2$.

Appendix B. Nonlocal solitary waves and embedded solitons in the perturbed KdV5 equation

When $\varepsilon = 0$, Eq. (3.4) has a parametric family of solitons

$$v_0(\zeta) = \frac{3}{2}k^2 \operatorname{sech}^2 \frac{k\zeta}{2}, \tag{B.1}$$

where $c = bk^2 + k^4$, and $k^2 = -(3-b)/10$.

Therefore, in terms only of b it can be written in a standard squared hyperbolic secant form for $b > 3$

$$v_0(\zeta) = -\frac{3}{20}(3-b)\operatorname{sech}^2 \frac{\sqrt{-(3-b)}\zeta}{2\sqrt{10}}, \tag{B.2}$$

and, for $b < 3$, in the alternative 'gap soliton-like' form

$$v_0(\zeta) = -\frac{3}{20}(3-b)\sec^2 \frac{\sqrt{3-b}\zeta}{2\sqrt{10}}. \tag{B.3}$$

Also, eliminating k in terms of b yields

$$c = \frac{1}{100}\left(11b^2 - 36b + 9\right). \tag{B.4}$$

Note that $c_{min} = -0.2045$ at $b = 18/11$, and so the graph of c as a function of b, and the corresponding solution (B.3), falls in either of regions 3 or 4 of Fig. 1(a). See Fig. B.13:

Also note that the parametric family of solitons

$$v_0(\zeta) = \frac{1}{2}k^2 \operatorname{sech}^2 \frac{k\zeta}{2}, \tag{B.5}$$

considered in [10] does not belong within our family of solutions for any b value, and is a disjoint family which solves Eq. (3.4) for $\varepsilon = 0$ only for the single special value of the dispersion coefficient $b = 1$ considered in that paper. As we shall see, this will lead to entirely distinct families of embedded solitary waves from those derived in [10], even though our techniques are direct generalizations of those developed in that seminal treatment.

For $0 \neq \varepsilon \ll 1$, we propose the solution v of Eq. (3.4) as a regular perturbation series (4.1). If we substitute (4.1) back into (3.4)–(3.5), we obtain a family of equations corresponding to the different powers of ε. At order ε^0, one obtains an equation for $v_0(\zeta)$, which reproduces Eq. (3.4) for $\varepsilon = 0$.

At order ε, the equation for $v_1(\zeta)$ is

$$Lv_1 = G(v_0), \tag{B.6}$$

where the linear operator L is

$$L = \frac{d^4}{d\zeta^4} + b\frac{d^2}{d\zeta^2} - c + 6v_0 + 10v_0'' + 30v_0^2 + 10\frac{d}{d\zeta}\left(v_0\frac{d}{d\zeta}\right), \tag{B.7}$$

which is self-adjoint.

To solve the inhomogeneous equation (B.6), we must determine the solutions of the homogeneous equation $L\Psi = 0$, which is a fourth order equation and, therefore, has four linearly independent solutions. One of them, the localized solution, is easy to find: it is $\Psi_1 = v_0'$, which is antisymmetric. The nonlocal solutions are harder to find, and the reader can check the process to find the other two bounded solutions in [11,32]. They are:

$$\begin{aligned}\Psi_2 = \frac{\gamma}{4}\Bigg\{&\sin p\zeta\left[105k^2p + 4p^3 - 105k^2p\tanh^2\frac{k\zeta}{2}\right]\\ &+ \cos p\zeta\left[(-18k + 720k^3 + 30kp^2 + 15kb)\tanh\frac{k\zeta}{2}\right.\\ &\left.- 210k^3\tanh^3\frac{k\zeta}{2}\right]\Bigg\},\end{aligned} \tag{B.8}$$

and

$$\begin{aligned}\Psi_3 = \frac{\gamma}{4}\Bigg\{&\sin p\zeta\left[(-18k + 720k^3 + 30kp^2 + 15kb)\tanh\frac{k\zeta}{2}\right.\\ &\left.- 210k^3\tanh^3\frac{k\zeta}{2}\right]\\ &- \cos p\zeta\left[105k^2p + 4p^3 - 105k^2p\tanh^2\frac{k\zeta}{2}\right]\Bigg\},\end{aligned} \tag{B.9}$$

where p is defined via the equation $c = p^4 - bp^2$, and γ is a normalization constant. The fourth solution is unbounded, and will not be relevant in the following analysis.

Also, notice that Ψ_2 is antisymmetric and Ψ_3 is symmetric, and so at infinity, the asymptotic behavior of these solutions is

$$\Psi_2 \to \sin(p\zeta \pm \phi_2), \qquad \zeta \to \pm\infty, \tag{B.10}$$

$$\Psi_3 \to \pm\sin(p\zeta \pm \phi_3), \qquad \zeta \to \pm\infty, \tag{B.11}$$

where

$$\begin{aligned}\tan\phi_2 &= \frac{4p^3}{-18k + 510k^3 + 30kp^2 + 15kb},\\ \tan\phi_3 &= \frac{-18k + 510k^3 + 30kp^2 + 15kb}{4p^3},\end{aligned} \tag{B.12}$$

and it is easy to see that

$$\phi_3 - \phi_2 = \frac{\pi}{2}. \tag{B.13}$$

At this point we can solve the inhomogeneous equation (B.6). If v_1 should be localized, the inhomogeneous term $G(v_0)$ must be orthogonal to the bounded solutions Ψ_1, Ψ_2 and Ψ_3 of the homogeneous equation, i.e.,

$$\langle G(v_0), \Psi_1\rangle = \langle G(v_0), \Psi_2\rangle = \langle G(v_0), \Psi_3\rangle = 0, \tag{B.14}$$

where the inner product $\langle *, *\rangle$ is defined in the usual way

$$\langle f(x), g(x)\rangle \equiv \int_{-\infty}^{\infty} f(x)g(x)dx. \tag{B.15}$$

By looking at Eqs. (3.5) and (B.1), it is clear that $G(v_0)$ is symmetric. Therefore, it will be orthogonal to Ψ_1 and Ψ_2; however, in general it is not orthogonal to Ψ_3. With the help of Mathematica one can get the expression

$$\begin{aligned}\langle G(v_0), \Psi_3\rangle = \frac{3\gamma\pi}{40}p^2(k^2 + p^2)\Big\{&-2a_3(4k^2 + p^2)(-6 + 125k^2 + p^2 + 5b)\\ &- a_1\left(270k^4 - 4p^2(-6 + p^2 + 5b) + k^2(6 - 476p^2 - 5b)\right)\\ &+ a_2\left(-1270k^4 + 2p^2(-6 + p^2 + 5b) + k^2(42 + 218p^2 - 35b)\right)\Big\}\operatorname{csch}\frac{p\pi}{k},\end{aligned} \tag{B.16}$$

which is, indeed, generally nonzero. Hence, the v_1 solution is nonlocal, and so is $v(\zeta)$.

References

[1] P.G. Drazin, R.S. Johnson, Solitons: An Introduction, Cambridge University Press, Cambridge, 1992.

[2] G.B. Whitham, Linear and Nonlinear Waves, Wiley, New York, 1974, http://dx.doi.org/10.1002/eqe.4290040514.

[3] R.K. Dodd, J.C. Eilbeck, J.D. Gibbon, H.C. Morris, Solitons and Nonlinear Wave Equations, Academic Press, London et al, 1982, http://dx.doi.org/10.1002/zamm.19850650811.

[4] H. Michallet, E. Barthélemy, Experimental study of interfacial solitary waves, J. Fluid Mech. 366 (1998) 159–177, http://dx.doi.org/10.1017/S002211209800127X.

[5] P.J. Olver, Hamiltonian perturbation theory and water waves, Contemp. Math. 28 (1984) 231–249.

[6] R. Grimshaw, E. Pelinovsky, O. Poloukhina, Higher-order Korteweg-de Vries models for internal solitary waves in a stratified shear flow with a free surface, Nonlinear Process. Geophys. 9 (2002) 221–235, http://dx.doi.org/10.5194/npg-9-221-2002.

[7] A. Karczewska, P. Rozmej, E. Infeld, Shallow-water soliton dynamics beyond the Korteweg-de Vries equation, Phys. Rev. E 90 (1) (2014) 012907, http://dx.doi.org/10.1103/physreve.90.012907.

[8] K.A. Gorshkov, L.A. Ostrovsky, V.V. Papko, Interactions and bound states of solitons as classical particles, Sov. Phys.—JETP 44 (2) (1976) 306–311.

[9] K.R. Khusnutdinova, Y.A. Stepanyants, M.R. Tranter, Soliton solutions to the fifth-order Korteweg-de Vries equation and their applications to surface and internal water waves, Phys. Fluids 30 (2) (2018) 022104, http://dx.doi.org/10.1063/1.5009965.

[10] J. Yang, Dynamics of embedded solitons in the extended Korteweg-de Vries equations, Stud. Appl. Math. 106 (3) (2001) 337–365, http://dx.doi.org/10.1111/1467-9590.00169.

[11] S.R. Choudhury, R. Alfonso Rodriguez, Perturbative and reversible systems approaches to new families of embedded solitary waves of a generalized fifth-order Korteweg-de Vries equation, Partial Differ. Equ. Appl. Math. 5 (2022) 100314, http://dx.doi.org/10.1016/j.padiff.2022.100314.

[12] A.R. Champneys, Homoclinic orbits in reversible systems and their applications in mechanics, fluids and optics, Physica D 112 (1998) 158–186, http://dx.doi.org/10.1016/S0167-2789(97)00209-1.

[13] J.P. Boyd, Weakly non-local solitons for capillary-gravity water waves: Fifth-degree Korteweg de Vries equation, Physica D 48 (1991) 129–146, http://dx.doi.org/10.1016/0167-2789(91)90056-F.

[14] R. Grimshaw, Exponential asymptotics and generalized solitary waves, in: Steinr (Ed.), Asymptotic Methods in Fluid Mechanics: Survey and Recent Advances, in: CISM Courses and Lectures, vol. 523, Springer, Vienna, 2010, pp. 71–120.

[15] Y. Pomeau, A. Ramani, B. Grammaticos, Structural stability of the Korteweg-de Vries solitons under a singular perturbation, Physica D 31 (1988) 127–134, http://dx.doi.org/10.1016/0167-2789(88)90018-8.

[16] T.R. Akylas, T.S. Yang, On short-scale oscillatory tails of long-wave disturbances, Stud. Appl. Math. 94 (1) (1995) 1–20, http://dx.doi.org/10.1002/sapm19959411.

[17] S. Kichenassamy, P.J. Olver, Existence and non-existence of solitary wave solutions to higher-order model evolution equations, SIAM J. Math. Anal. 23 (5) (1992) 1141–1166, http://dx.doi.org/10.1137/0523064.

[18] P. Saucez, A. Vande Wouwer, P.A. Zegeling, Adaptive method of lines solutions for the extended fifth-order Korteweg-de Vries equation, J. Comput. Appl. Math. 183 (2005) 343–357, http://dx.doi.org/10.1016/j.cam.2004.12.028.

[19] S. Roy Choudhury, G. Gambino, Convergent analytic solutions for homoclinic orbits in reversible and non-reversible systems, Nonlinear Dynam. 73 (3) (2013) 1769–1782, http://dx.doi.org/10.1007/s11071-013-0902-z.

[20] K.R. Khusnutdinova, Y.A. Stepanyants, M.R. Tranter, Soliton solutions to the fifth-order Korteweg-de Vries equation and their applications to surface and internal water waves, Phys. Fluids 30 (2) (2018) http://dx.doi.org/10.1063/1.5009965.

[21] G. Iooss, K. Kirchgässner, Water waves for small surface tension: An approach via normal form, Proc. Roy. Soc. Edinburgh Sect. A 122 (3–4) (1992) 267–299, http://dx.doi.org/10.1017/S0308210500021119.

[22] E. Lombardi, Homoclinic orbits to small periodic orbits for a class of reversible systems, Proc. Roy. Soc. Edinburgh Sect. A 126 (5) (1996) 1035–1054, http://dx.doi.org/10.1017/S0308210500023246.

[23] E. Lombardi, Orbits homoclinic to exponentially small periodic orbits for a class of reversible systems. Application to water waves, Arch. Ration. Mech. Anal. 137 (1997) 227–304, http://dx.doi.org/10.1007/s002050050029.

[24] A.R. Champneys, B.A. Malomed, Moving embedded solitons, J. Phys. A: Math. Gen. 32 (50) (1999) L547–L553, http://dx.doi.org/10.1088/0305-4470/32/50/103.

[25] K. Kirchgässner, Nonlinearly resonant surface waves and homoclinic bifurcation, Adv. Appl. Mech. 26 (1988) 135–181, http://dx.doi.org/10.1016/S0065-2156(08)70288-6.

[26] C. Elphick, E. Tirapegui, M. Brachet, P. Coullet, G. Iooss, A simple global characterization for normal forms of singular vector fields, Physica D 29 (1987) 95–127, http://dx.doi.org/10.1016/0167-2789(87)90049-2.

[27] G. Iooss, M.C. Peroueme, Perturbed homoclinic solutions in reversible 1: 1 resonance vector fields, J. Differential Equations 102 (1993) 62–88, http://dx.doi.org/10.1006/jdeq.1993.1022.

[28] G. Iooss, K. Kirchgassner, Bifurcation d'ondes solitaires en présence d'une faible tension superficielle, C. R. Acad. Sci., Paris I 311 (1990) 265–268.

[29] B. Buffoni, M.D. Groves, A multiplicity result for solitary gravity-capillary water waves via critical-point theory, Arch. Ration. Mech. Anal. 146 (1999) 183–220, http://dx.doi.org/10.1007/s002050050141.

[30] J. Härterich, Kaskaden homokliner orbits in reversiblen dynamischen systemen (Master's thesis), Universität Stuttgart, 1993.

[31] J. Härterich, Cascades of reversible homoclinic orbits to a saddle-focus equilibrium, Physica D 112 (1998) 187–200.

[32] J. Yan, Y. Tang, Direct approach to the study of soliton perturbations, Phys. Rev. E 54 (1996) 6816–6824, http://dx.doi.org/10.1103/PhysRevE.54.6816.